AEROSOL INVESTIGATIONS

FOREWORD

H. F. Johnstone
Technical Director, Contract AT(30-3)-28

Engineering Experiment Station
University of Illinois
Urbana, Illinois

At the air Cleaning Conference at Ames in September 1952, reports were given by the Illinois group on the fundamental investigations on aerosols which were being studied at that time. The following reports have been prepared by the members of the research staff to show the status of the current work.

Most of the work on the contract at Illinois is carried on by graduate students in Chemical Engineering. These men are being trained in research methods and in the applications of physics and mathematics to aerosol technology. By working as a group, they have the advantages of using standardized procedures and of group discussions. Of those who have completed their work, several have taken positions in university and industrial laboratories where they have continued their interest in fundamental and practical aerosol problems. Because of the need for greater knowledge in this field of science in this country, it is felt that the training of scientists is one of the important contributions of the work.

All of the work on the project is not supported directly by the AEC contract. A part of it is being carried on in the regular graduate thesis program in Chemical Engineering. The work of Mr. H. F. Kraemer on properties of charged aerosols falls in this category. During the past year, the Chemical Corps, through Contract No. DA-18-108-CML-4789, has expanded the investigation on the theory of filtration of very small particles. This work is being carried on by Dr. C. Y. Chen, a Research Associate in the Engineering Experiment Station. Since these studies are related to the fundamental properties of aerosols, they are summarized here for the interest of those in the AEC who are concerned with aerosol work.

During the year, one phase of the theoretical studies and one experimental program were completed. The results were reported in two technical reports as follows:

> "I. The Role of Particle Diffusion and Interception in Aerosol Filtration; II. Determination of the Drag on a Cylindrical Fiber at Low Reynolds Number". Technical Report No. 8, Serial No. SO-1009, January 1, 1953; cf. also errata sheet issued with Technical Report No. 9.

"Particle Size Distribution in Hygroscopic Aerosols". Technical Report No. 9, Serial No. SO-1010, May 1, 1953. This work was presented at the Symposium on Fumes and Mists at the meeting of the American Institute of Chemical Engineering in St. Louis, in December, 1953; the paper was published in Chemical Engineering Progress Symposium Series.

TURBULENT DEPOSITION AND THE BEHAVIOR OF DEPOSITS OF SOLID PARTICLES

by

S. K. Friedlander, Research Assistant

When a gas containing particles flows in turbulent motion past a surface, some of the particles are deposited even though there is no net velocity in the direction of the surface. This turbulent deposition results from the fluctuating velocity component normal to the collecting area. It occurs in the movement of aerosols through straight ducts, through diffuser sections, and on any body whose boundary layer becomes turbulent when passing through a gas containing particles. It undoubtedly contributes to removal in such devices as cyclones and cyclone scrubbers operated at high levels of turbulence.

In essence, turbulent deposition is a form of inertial removal in which sudden gusts of fluid move towards the surface, change their direction, and thereby cast out the particles which they carry. There is no real distinction between this phenomenon and impaction. For example, when a turbulent gas flows past a flat surface, the motion of the eddies toward the surface can be thought of as a series of impactions on flat plates, for which we have experimental and theoretical data. Similarly, a spherical water droplet moving out of phase with an eddy probably removes particles from the surrounding aerosol by impaction. The difficulty in a theoretical analysis of turbulent impaction derives from our inability in most cases to characterize the velocity and scale of the turbulence. However, since impaction is the mechanism of deposition, the important parameter should be the inertial group (2):

$$\Psi = \frac{C \rho_p V_e}{18 \mu d_e} d_p^2$$

where C = Cunningham correction factor

ρ_p = particle density

V_e = eddy velocity

d = some characteristic length

μ = gas viscosity

d_p = particle diameter

By studying the effect of these variables on turbulent deposition, one should at least be able to correlate experimental data, although prediction of results from theory is more difficult.

EQUIPMENT

In order to study turbulent deposition and the behavior of deposits of solid particles, the equipment outlined in Fig. 1 was set up. The aerosol employed was carbonyl iron powder (Grade SF) manufactured by the Antara Chemicals Division of the General Dyestuff Corporation. According to the manufacturer's catalog, the mass median diameter of the particles was 3 microns with a geometric standard deviation of about 1.4. This material was chosen because the particles are quite spherical, easy to see under the microscope, and easy to disperse. Tests disclosed that about 10 percent of the particles were agglomerates and most of these were doublets. It has the disadvantage of a density (7.8 g./cc.) considerably higher than that of the usual aerosol particles.

The iron powder was placed in a brass "boat", about 1 1/2 feet long, which was pushed forward by a threaded steel rod of similar length attached to the shaft of a small 10 rpm. motor. In this way, the powder was fed at a steady rate to an atomizing nozzle. In order to remove the larger particles and increase the homogeneity of the aerosol, a 1-inch cyclone was installed after the atomizer and before the mixing chamber leading to the sampling tube. The aerosol concentration was determined by passing a known volume of air from the sampling tube through a Millipore filter (Lovell Chemical Co.). The main body of air passed through a rotameter and was expelled from the system by a Roots-Connersville blower.

Two sampling tubes have been used up to the present, one 5.4 mm. I.D. and the other 13 mm. I.D. Both tubes were of thin wall Pyrex, and each was ground at one point to permit observation of the inner wall using a microscope with an oil immersion technique. The observation points for the 5.4 and 13 mm. tubes were placed 50 and 30 diameters, respectively, from the entrance, to minimize entrance effects. In order to restrict the tests to a known particle size, only those particles with diameters ranging from about 0.6 to 1 micron were counted both on the Millipore filter (for determining concentration) and on the tube wall (for determining deposition), and a mean particle size of 0.8 microns was assumed.

RESULTS

In general, when particles deposit on a surface, two stages can be recognized. In the first, the individual aerosol particles scatter about the surface and, unless the velocity is high (above 100 ft./sec.), there is little re-entrainment. In the second stage, as a result of increased deposition clumps of particles appear and parts of these may break away, even at moderate gas velocities. Since the first stage seemed more amenable to investigation, it has received most attention in our experimental work.

The deposition rate was characterized by defining a particle transfer coefficient, k, with the dimensions of cm./min.

$$k = N/c$$

where N = deposition rate, particles/(cm.^{2})(min.)

c = particle concentration, particles/cc.

A plot of this coefficient as a function of velocity for both experimental tubes is shown in Fig. 2. The data for both tubes fall essentially along the same line. Most evident, however, is the extreme effect of increasing velocity on the transfer rate which is proportional to V^5. The cause of this extreme velocity dependence is not certain although a somewhat similar effect is found for impaction on flat plates (1). In passing, it should be noted that at the very high velocity (180 ft./sec.) in the smaller tube, 2.5 percent of the particles were removed per inch of duct length.

Larger particles (those above 2 or 3 microns) appeared to have a greater tendency to deposit than the smaller sizes and this tendency would be predicted from the impaction mechanism; however, the larger particles are also reentrained considerably faster since they project into the higher velocity regions of flow. Thus at high velocities, the initial deposit consisted mostly of smaller particles. This effect has also been noted by Rumpf (3).

REFERENCES

1. Ranz, W. E. and Wong, J. B., "Jet Impactors for Determining the Particle Size Distributions of Aerosols", Eng. Expt. Sta., University of Illinois, Tech. Report No. 4, Serial No. SO-1004, July 31, 1951.
2. Ranz, W. E. and Wong, J. B., "Impaction of Dust and Smoke Particles", Ind. Eng. Chem. 44, 1371 (1952).
3. Rumpf, H., "The Formation of Finely Distributed Substances on the Walls of Pipe Lines", Chemie Ingenieur Technik, Part 6, p. 317, (1953).

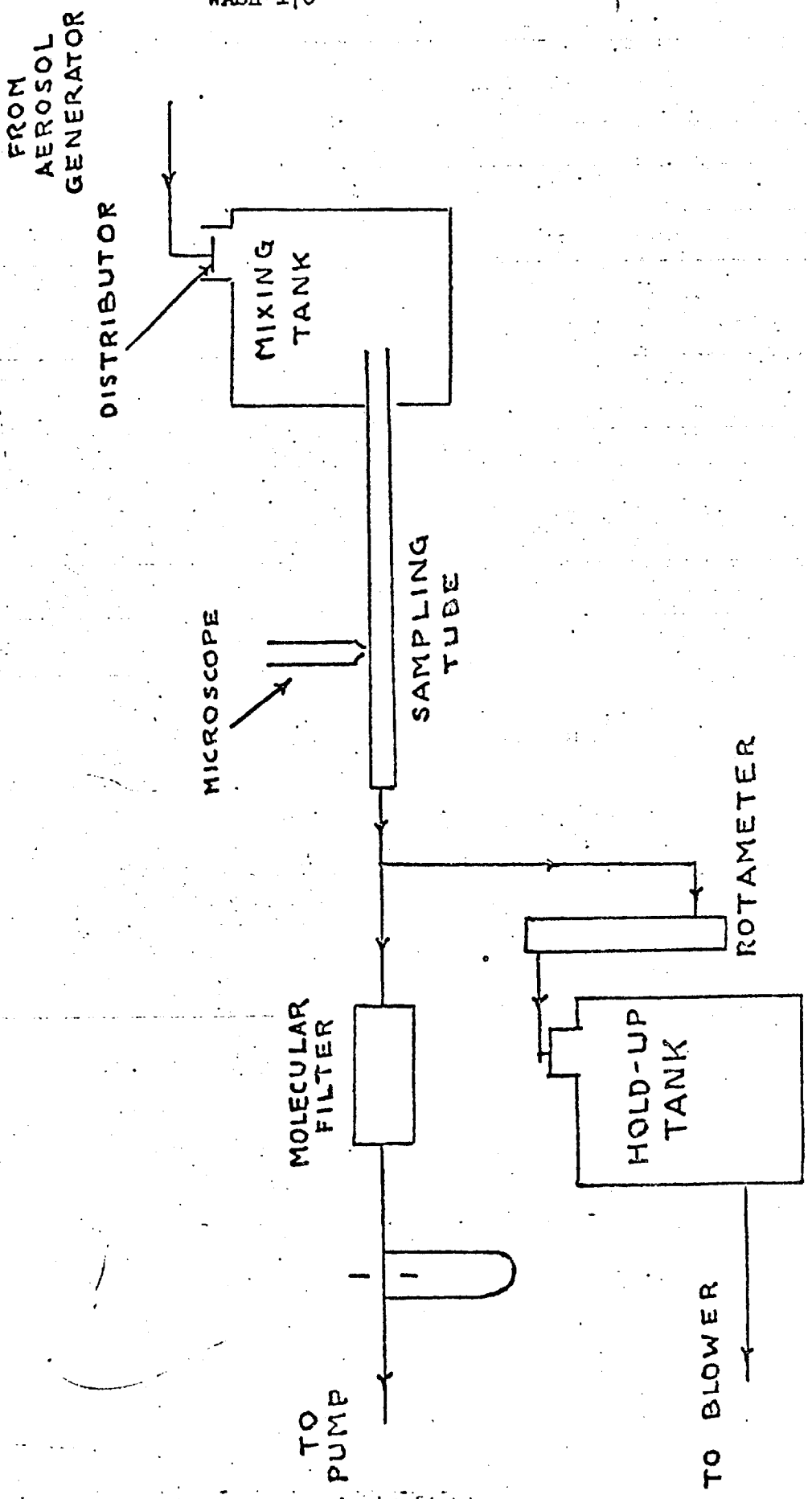

FIG. 1
APPARATUS FOR MEASUREMENT
OF TURBULENT DEPOSITION

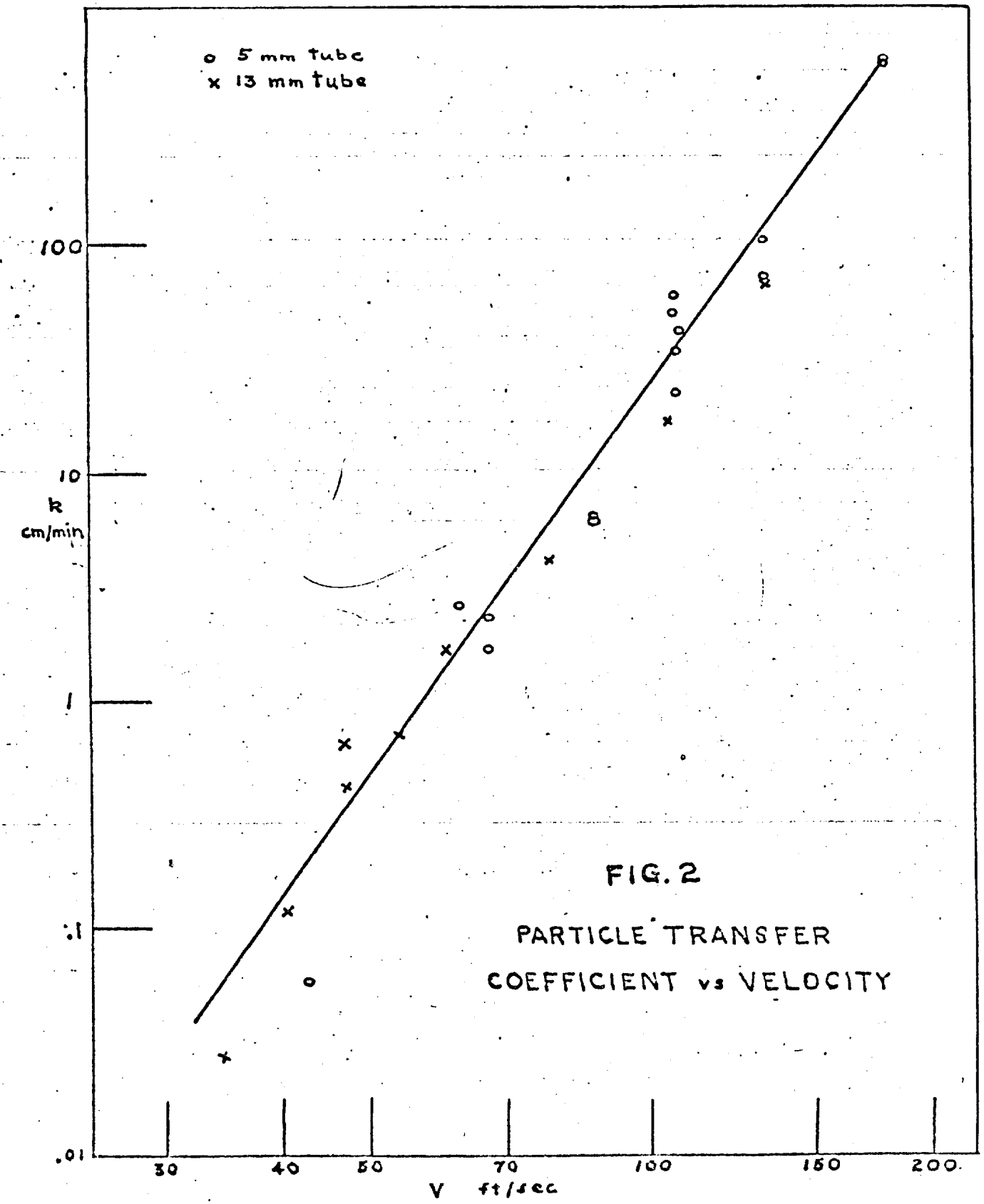

FIG. 2

PARTICLE TRANSFER COEFFICIENT vs VELOCITY

COLLECTION OF AEROSOLS BY FIBER MATS

by

James B. Wong, Research Assistant

A major class of aerosol filters consists of beds of individual fibers. The efficiency of collection and the pressure drop are the important practical considerations in the design of these fibrous filters. An understanding of the mechanisms by which the particles are collected on isolated cylinders and the flow pattern around the cylinders is fundamental in the design. In view of the several mechanisms of particle collection, it is best to investigate them individually. In the present work, emphasis is placed on the mechanism of inertial impaction. This mechanism takes place when a particle approaching a fiber crosses the streamlines because of its inertia and strikes the surface of the fiber.

The work is divided into two parts. Part I deals with the impaction of aerosol particles on single cylinders (metallic wires) with axes perpendicular to the direction of the aerosol flow. Part II deals with the collection efficiency and the pressure drop of fiber mats.

PART I. IMPACTION ON SINGLE CYLINDERS (METALLIC WIRES)

The theory of impaction of particles on circular cylinders with their axes perpendicular to the direction of flow has been studied by Sell (12), Albrecht (1), Langmuir and Blodgett (9), Landahl and Herrmann (7), and Davies (3). Davies indicates that the efficiency of inertial impaction should be a function of the inertial parameter Ψ and the Reynolds Number based on the diameter of the cylinder. Albrecht, and Langmuir and Blodgett predict on theoretical grounds that a critical value of Ψ exists below which inertial impaction does not occur. Albrecht gives 0.09 whereas Langmuir and Blodgett give 0.0625 for the critical value. The other authors do not indicate such a critical value.

Since experimental verification of the theoretical conclusions is lacking, the present work was undertaken with the purpose of ascertaining the correct function of the efficiency of inertial impaction and the existence or non-existence of the critical value of Ψ.

One-mil and 3-mil platinum wires and 2-mil and 4-mil tungsten wires were used as the circular cylinders. The average diameters from measurements under the microscope, were 29.0, 82.6, 53.1, and 105.7 microns, respectively, with a maximum deviation from the average of less than 9 percent. Homogeneous sulfuric acid aerosols were used in the experiments. The aerosols were generated with a condensation aerosol generator similar to that used by Sinclair and LaMer (13). The particle sizes were measured with a calibrated Owl (No. G-2) obtained from the U. S. Army Chemical Corps. The acid concentration of the aerosol was determined by collecting a weighable quantity of the particles in the cup of a high velocity impactor (11) and analyzing the contents of the cup by titrating

with 0.1 N sodium hydroxide solution.

The experimental procedure included generating a homogeneous sulfuric acid aerosol of the desired particle size, impacting the aerosol particles on the wire which was perpendicular to the direction of the aerosol flow, collecting the remaining particles in a glass fiber filter train, and analyzing the amount of acid collected on the wire. In order to collect enough acid on the wire for accurate analysis, a brass drum which could be rotated was attached to the top of the impacting nozzle and about four feet of wire was unwound from the drum to pass through the nozzle during a run. The wire, after being exposed to the aerosol at the nozzle throat, was passed down into an 8-mm. Pyrex glass tube. At the end of the run, conductivity water was used to wash off the acid particles impacted on the wire and the quantity of acid was determined by measuring the concentration of the wash solution with a precision conductivity bridge and dip cell which accurately indicated concentrations as low as 10^{-6} N. From the quantity of acid impacted on the wire and the total amount of acid in the aerosol passing the nozzle, the efficiency of impaction could be calculated.

Figure 1 shows the experimental impaction efficiencies on the four wires. The range of variables represented are: D_p, diameter of aerosol particles, 0.56 to 1.40 microns; V_o, velocity of the aerosol stream passing the wires, 400 to 5100 cm./sec.; and Reynolds Number ($N_{Re} = D_c V_o \rho/\mu$) based on the measured wire diameters, 13.0 to 330. The density of the sulfuric acid particles, ρ_p, was substantially constant with an average of 1.48 g./cc. C is the Cunningham correction factor and μ is the viscosity of the gas.

In the ranges of particle diameter and aerosol stream velocity employed in the experiments, collection due to the Brownian diffusion was negligible. Collection by electrostatic forces was improbable since both the aerosol particles and the wires were uncharged. Gravity settling should also be unimportant with the wires in the vertical position. The collection due to interception was estimated to be less than 10 percent of the total collection in all cases, and thus had very little effect on the shape or position of the resulting efficiency curve. The curve drawn through the points in Figure 1, therefore, represents the experimental efficiencies of inertial impaction.

The experimental curve is S-shape, characteristic of the inertial impaction mechanism on surface and body collectors. It indicates a critical value of $\sqrt{\Psi}$ of approximately 0.25, below which impaction does not occur. At high values of the inertial parameter, the curve appears to be asymptotic to the value of $\eta_I = 1$. The accuracy and reliability of the results depend largely on the homogeneity of the particle size and the accuracy of the particle size measurements. The impaction efficiencies were reproducible in terms of $\sqrt{\Psi}$, in view of the ten-fold variation in velocity, the three-fold variation in particle size, and the insensitivity of the Owl for detecting small variations in the particle size.

Comparisons of the data for the two platinum wires show that the higher the Reynolds Number, the higher is the impaction efficiency for the same value of the inertial parameter. The same observation can be made on the two tungsten wires. This agrees with the theoretical conclusions. Comparison of the data for the 1-mil platinum wire with those for the 2-mil tungsten wire, and the data for the 3-mil platinum wire with those for the 4-mil tungsten wire, however, show opposite effects of the Reynolds Number, i.e., the impaction efficiencies on the 3-mil wire at lower values of the Reynolds Number are generally higher than those on the 4-mil wire for corresponding value of $\sqrt{\Psi}$. The explanation of this is not apparent. When these wires were observed under the microscope, it was noted that the surface of the platinum wire was much smoother than that of

the tungsten wire. Possibly the aerosol particles adhere to the surface of the platinum better than to the tungsten wire.

Figure 2 is a plot of the experimental inertial impaction efficiency curve together with the various theoretical curves proposed. The experimental curve agrees closely with that calculated by Landahl and Herrmann based on Thom's flow lines for the Reynolds Number of 10, up to $\sqrt{\Psi} = 1.4$. For values of $\sqrt{\Psi}$ between 0.4 and 1.2, the data indicate impaction efficiencies somewhat smaller than those shown by the curve of Langmuir and Blodgett and considerably smaller than the values of Sell, and of Albrecht. This is to be expected since the curves of Langmuir and Blodgett, and Albrecht were based on the potential flow of an ideal fluid, and that of Sell was based on an observed flow pattern obtained at large values of the Reynolds Number on a 10 cm. cylinder. No comparison can be made with Davies' theoretical curve since it was based on viscous flow at a Reynolds Number of 0.2, far below the range attainable with the method used in the experiment.

For values of $\sqrt{\Psi}$ greater than about 1.4, the experimental efficiencies are higher than those according to the curves of Langmuir and Blodgett, and Landahl and Herrmann. The reason for this discrepancy is not entirely clear. One point to be noted is that, for high efficiencies of inertial impaction, i.e., efficiencies approaching unity, the particle trajectories must be nearly parallel to the direction of flow and the particles must cut across the streamlines upstream of the wire where the streamlines begin to spread. In step-wise calculations of particle trajectories, it is not practical to start the calculation more than a few diameters (of the collector) upstream. It is possible that errors introduced by this could cause the calculated impaction efficiencies in the high efficiency range to be lower than the correct values.

The critical value of $\sqrt{\Psi}$ at approximately 0.25 shown by the experimental impaction efficiencies agrees with the values of 0.3 and 0.25 explicitly stated by Albrecht, and Langmuir and Blodgett, respectively. The curve of Landahl and Herrmann also implies that the efficiency of inertial impaction is negligible at the value of $\sqrt{\Psi}$ less than 0.25.

PART II. COLLECTION EFFICIENCY AND PRESSURE DROP OF FIBER MATS

The theory of the collection of particles on fibrous filters has been studied by Albrecht (1), Langmuir (8), and Davies (3). Albrecht's theory is based on the potential flow of an ideal fluid, a condition very different from viscous flow which ordinarily takes place in these filters. Langmuir's theory takes into account only two mechanisms of collection, interception and Brownian diffusion. The experimental data of LaMer (6), and Ramskill and Anderson (10) show that the mechanism of inertial impaction also plays an important part in the collection efficiency of these filters. However, these authors have not evaluated this mechanism quantitatively. Davies' theory takes into account all of the major mechanisms of particle collection. He proposed an equation derived on theoretical grounds for the efficiency of the fibers in the filter. The present work was conducted with the purpose of evaluating quantitatively the mechanism of inertial impaction.

Pressure drop across fibrous media has been studied on the basis of the hydraulic radius concept of Kozeny (5) and Carman (2). Davies (3) studied the problem by dimensional analysis. Iberall (4) and Langmuir (8) derived theoretical equations for the pressure drop. The conclusions of these authors are not

in good agreement. Another object of the present work was to test the proposed equations experimentally.

By assuming (a) all fibers in the filter mat are perpendicular to the direction of flow; (b) the fibers do not interfere with each other; and (c) the ends of fibers have negligible effect, the following equations have been derived for the collection efficiency and the pressure drop of the fiber mat:

$$\eta \text{ mat} = 1 - (N_h/N_o) = 1 - e^{-\left(\frac{4\alpha\eta}{\pi D_f}\right) h} \quad (1)$$

$$\Delta P = \frac{2\rho V_o^2 \alpha h C_D}{\pi D_f} \quad (2)$$

where

η mat = collection efficiency of the fiber mat

N_h/N_o = fraction of particles penetrating the mat

α = fiber volume fraction, i.e., volume of fibers per unit volume of mat

D_f = diameter of fibers in the mat

h = thickness of the mat

ρ = density of the gas

V_o = volumetric velocity of the aerosol stream passing the mat

η = total efficiency of the single fiber

C_D = drag coefficient on the single fiber

In actual fiber mats, none of these assumptions is completely justified. The approach followed in the present work was to use the equations as bases for correlating the experimental data, incorporating all of the effects which were not already taken into account as an effective fiber efficiency, η_e, and an effective fiber drag coefficient, C_{De}, instead of η and C_D in the equations.

The fiber mats used in the present work were formed from three types of glass fibers made by Glass Fibers, Inc., Toledo, Ohio, unbonded "B" fibers, "450" yarns, and "150" yarns. The diameters of the fibers were measured under the microscope and were found to average 3.51, 6.24, and 9.57 microns, respectively. The mats were formed by Arthur D. Little, Inc., Cambridge, Massachusetts. Four bulk densities of approximately 1.0, 1.3, 1.6, and 2.0 g./cc. were formed from each type of fiber. The thickness of the mats ranged from 0.13 to 0.22 cm. Most mats were uniform after the binding agent had been burned off.

The experimental procedure was similar to that followed on the impaction of single wires. The aerosol was directed to pass the mat which was placed in a Lucite holder with the mat face perpendicular to the direction of flow and the pressure drop was measured by means of inclined and ordinary manometers. The collection efficiency of the mat was calculated from the quantities of acid collected on the mat and in the filter train following the mat as determined by titration with standard sodium hydroxide solution and by conductivity measurement.

Figure 3 shows the experimental collection efficiencies. The ranges of variables represented are: diameter of aerosol particles, 0.43 to 1.3 microns; volumetric velocity of aerosol stream passing mats, 17 to 260 cm./sec./ Reynolds Number based on the fiber diameter, 0.04 to 1.4; fiber volume fraction, 0.045 to 0.098; and thickness of mats, 0.13 to 0.40 cm. The collection efficiency on the mats ranged from 0.04 to 0.998.

In the experiments, Brownian diffusion, electrostatic attraction, and gravity settling were negligible. The best curves for the effective fiber efficiency through the points at the interception parameters ($R = D_p/D_f$) of 0.1, 0.2, and 0.3, therefore, represent the total efficiency of impaction, which includes the inertial impaction and interception efficiencies, and the effect of fiber interference, fiber ends, and non-uniformity on the total efficiency of impaction. At $\sqrt{\Psi}$ of approximately 0.4, inertial impaction becomes unimportant and interception becomes the controlling mechanism as shown by the flattening of the curves. This critical value of $\sqrt{\Psi}$ of 0.4 is between the values of 0.52 and 0.3 predicted by Langmuir and Albrecht, respectively. It is greater than the value of 0.2 obtained experimentally by Ramskill and Anderson. Figure 3 shows that the mechanism of inertial impaction can be represented quantitatively in terms of the effective fiber efficiency.

Figure 4 shows the experimental pressure drop data correlated on the basis of the effective fiber drag coefficient. The ranges of variables are the same as those described for the collection efficiencies since the measurements were taken simultaneously. The pressure drop across the fiber mats ranged from 0.3 to 30 cm. of water. The fiber volume fraction, α, has a marked effect on the effective fiber drag coefficient. The higher the volume fraction, the higher the effective fiber drag coefficient. The effective fiber drag coefficient can be predicted by means of a theoretical equation based on an idealized mat with its fibers equally oriented in the three perpendicular directions one of which is in the direction of flow and an empirical factor, $1 + 60\alpha^{1.8}/N_{Re}^{0.3}$. This correction factor agreed with previous conclusions in that the drag on the fiber increases with the fiber volume fraction and the drag decreases with the Reynolds Number. Curves for this equation for α of 0.08, 0.04, and zero are shown in the figure. The figure also shows the theoretical and semi-theoretical curves of Kozeny-Carman, Davies, Iberall, and Langmuir. Calculated for $\alpha = 0.06$, the average fiber volume fraction in the experiments. The Kozeny-Carman, Davies, and Langmuir equations all predict the effective fiber drag coefficient to be inversely proportional to the Reynolds Number, i.e., a straight line with a slope of -1 in this plot. The experimental data, however, show a definite curvature. This indicates that the equations of these authors, while applicable in a limited range of the Reynolds Number for particular types of fibrous media, are functionally incorrect. Iberall's theoretical equation ("Iberall I" in the figure) shows approximately the correct curvature. The reason that his equation predicts too high a pressure drop can be explained on the basis of his erroneous assumption that the drag force per unit length for fibers parallel to the direc-

tion of flow was greater than for fibers perpendicular to the flow. It is concluded that the pressure drop across fiber mats can be correlated on the basis of the effective fiber drag coefficient.

From Equations 1 and 2 and the results of the experimental work, the optimum fiber mat can be derived for filtration of aerosols in the range in which inertial impaction is the important mechanism of collection.

LITERATURE CITED

1. Albrecht, F., Physik, Z., 32, 48 (1931).
2. Carman, P. C., Trans. Inst. Chem. Eng., (London), 15, 150 (1937).
3. Davies, C. N., Proc. Inst. Mech. Engrs. (London), B 1, 185 (1952).
4. Iberall, A. S., J. Research Nat. Bur. Standards, 45, 398 (1950).
5. Kozeny, J., Wasserkraft u. Wasserwirk, 22, 67, 86 (1927).
6. LaMer, V. K., "Studies on Filtration of Monodisperse Aerosols", Columbia University, Final Report, N.Y.O. Rept. No. 512, March 31, 1951, A.E.C. Contract No. AT(30-1)-651.
7. Landahl, H. D., and Herrmann, R. G., J. Colloid Sci., 4, 103 (1949).
8. Langmuir, I., "Filtration of Aerosols and the Development of Filter Materials", O.S.R.D. Rept. No. 865, Sept. 4, 1942.
9. Langmuir, I., and Blodgett, K. B., "Mathematical Investigation of Water Droplet Trajectories", General Electric Research Laboratory, Schenectady, New York, Rept. No. RL 225, 1944-45.
10. Ramskill, E. A., and Anderson, W. L., J. Colloid Sci., 6, 416 (1951).
11. Ranz, W. E., and Wong, J. B., Arch. Ind. Hyg. Occupational Med., 5, 464 (1952).
12. Sell, W., Forsch. Gebiete Ingenieurw., 2, Forschungsheft, 347 (August, 1931).
13. Sinclair, D., and LaMer, V. K., Chem. Rev., 44, 245 (1949).

FIG. 1. EXPERIMENTAL EFFICIENCIES OF INERTIAL IMPACTION ON CIRCULAR CYLINDERS

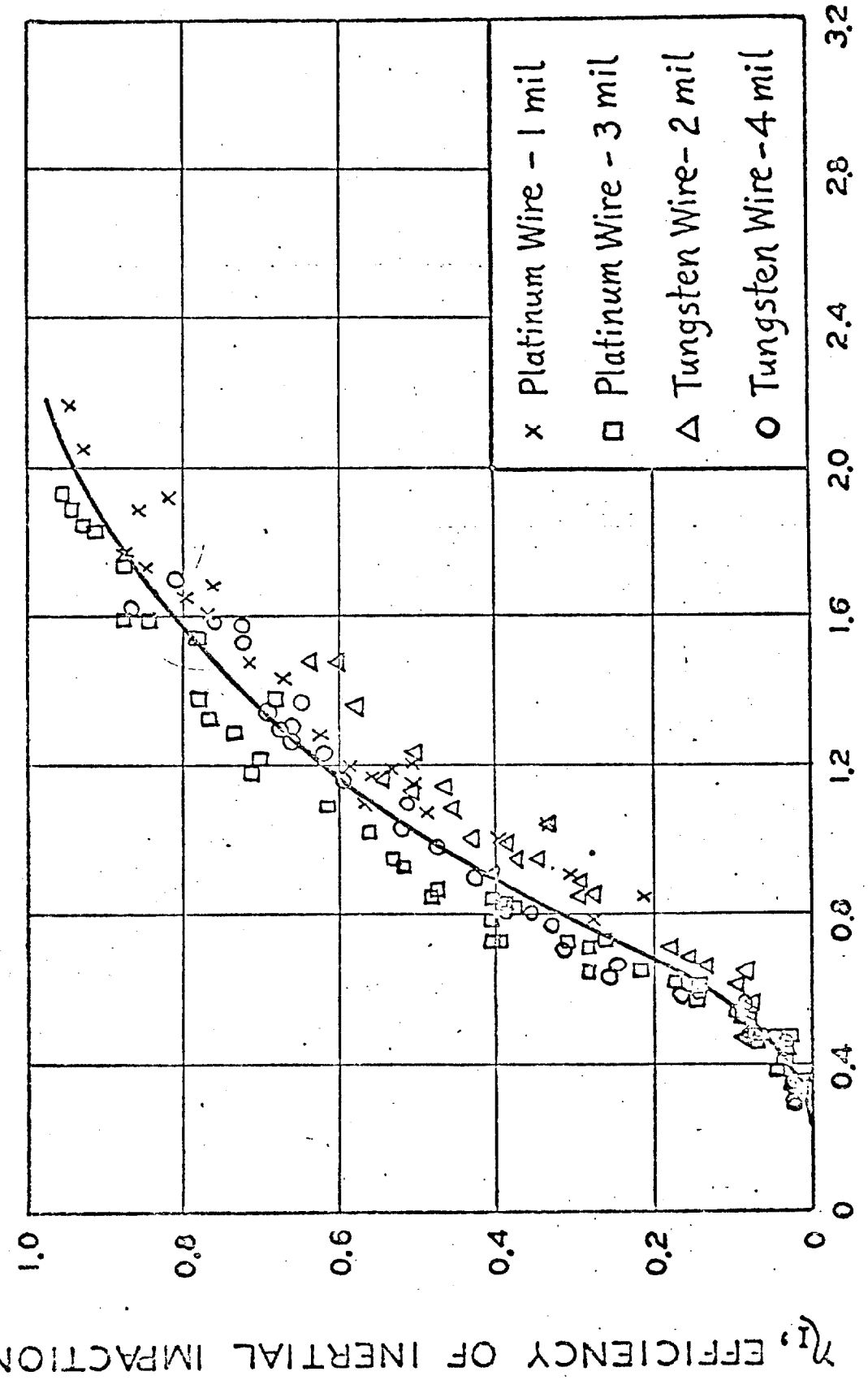

FIG. 2. COMPARISON OF THEORETICAL AND EXPERIMENTAL EFFICIENCIES OF INERTIAL IMPACTION ON CIRCULAR CYLINDERS

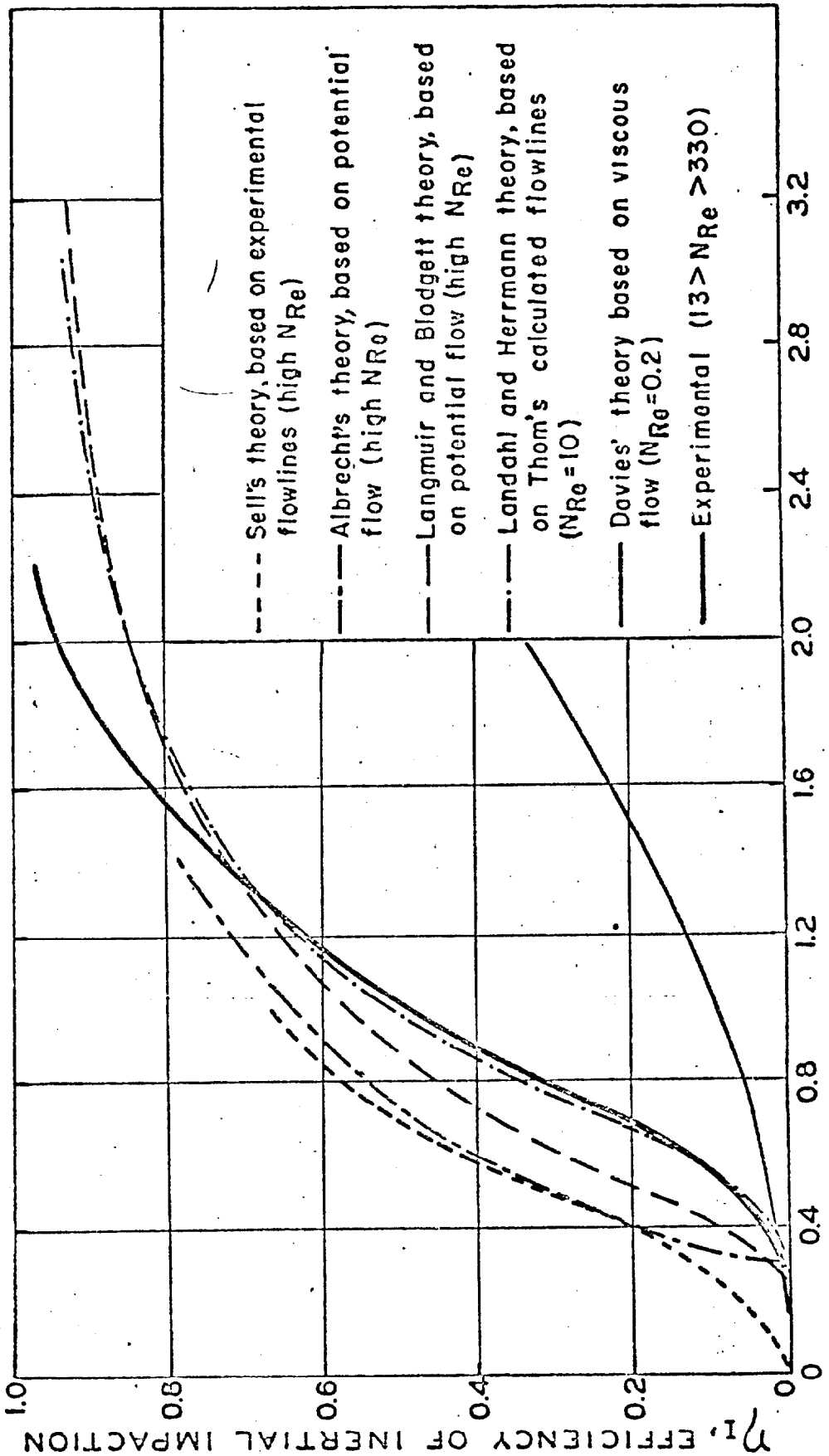

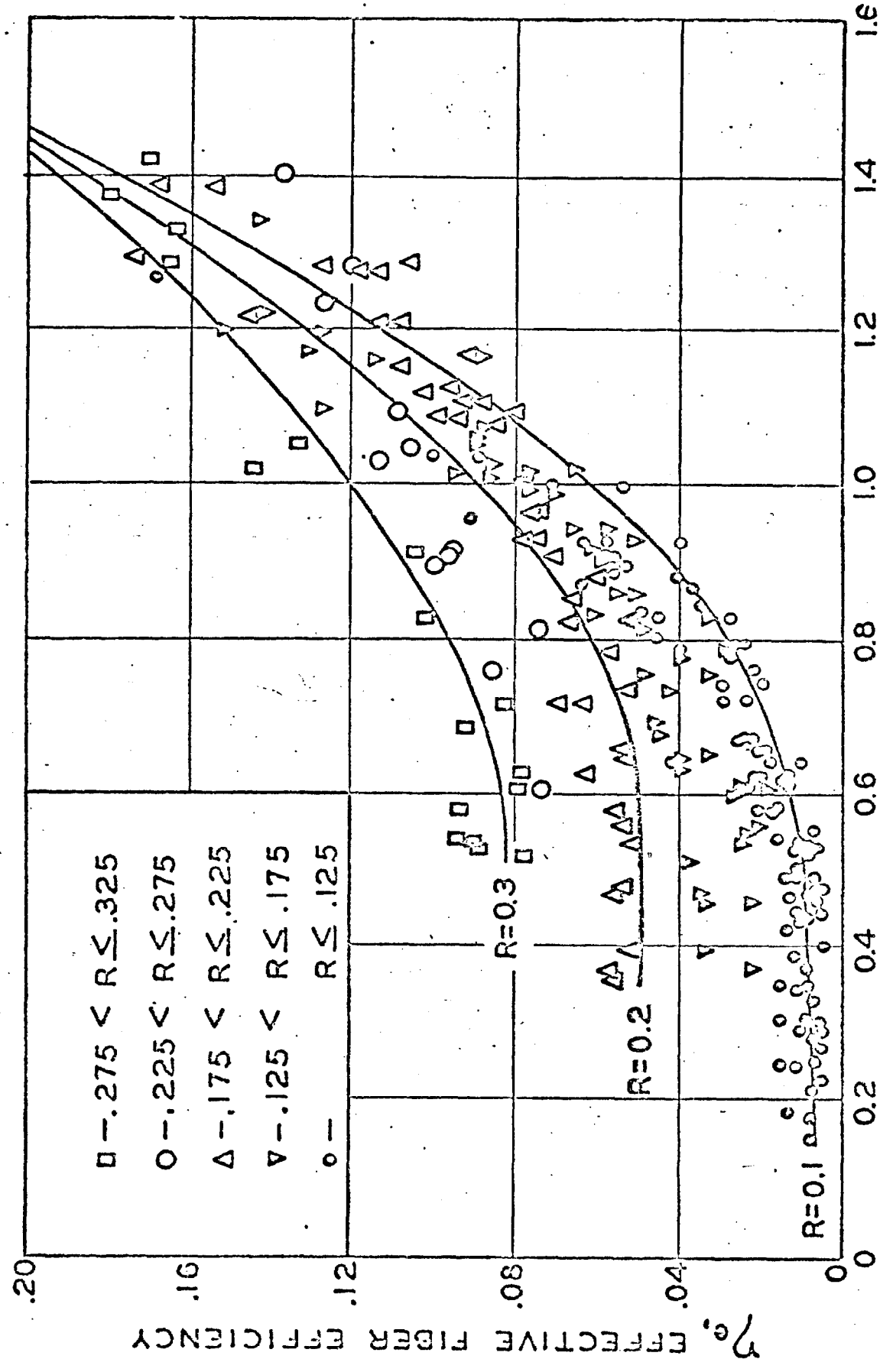

FIG. 3. EXPERIMENTAL EFFECTIVE FIBER EFFICIENCIES

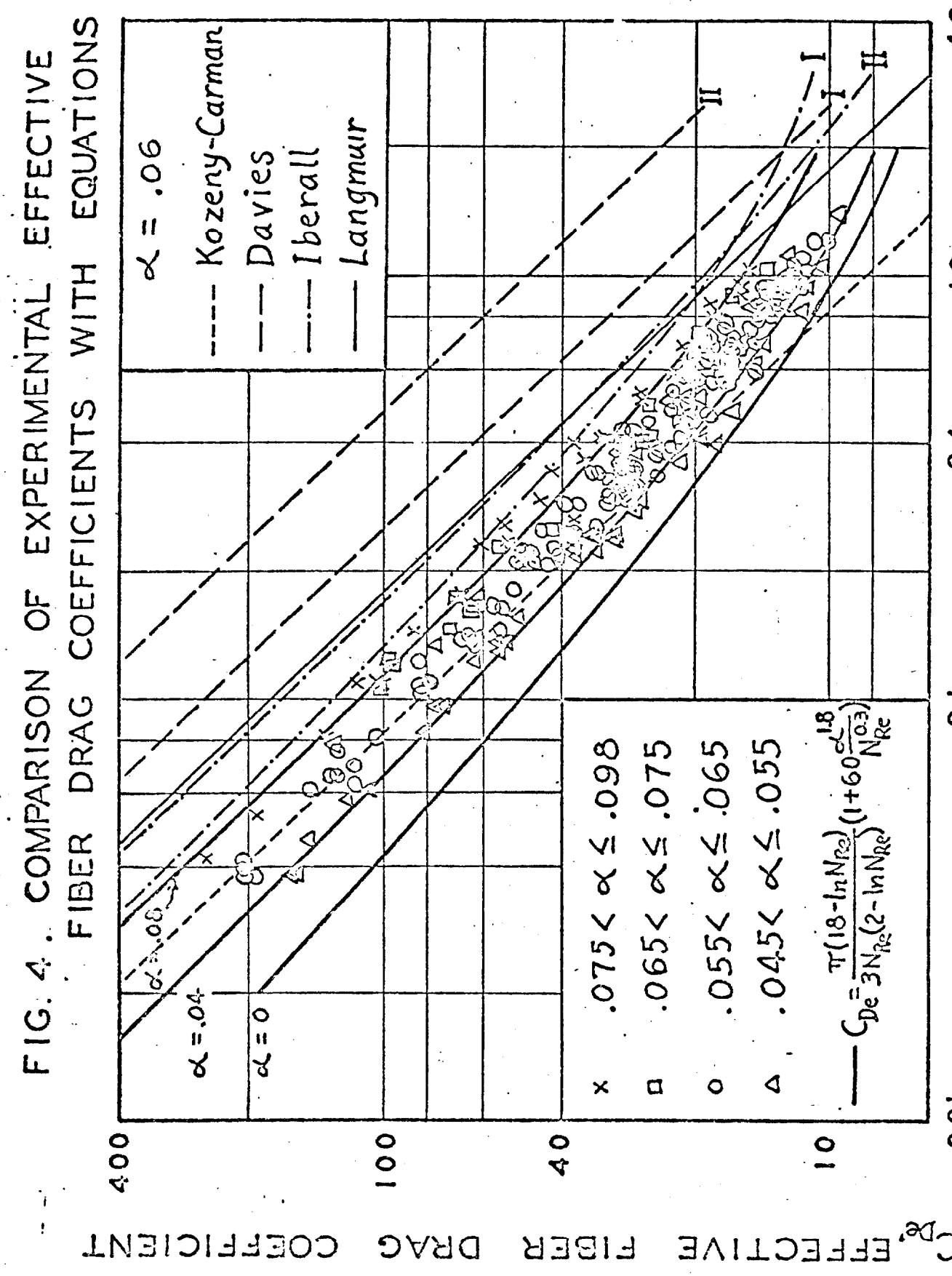

FIG. 4. COMPARISON OF EXPERIMENTAL EFFECTIVE FIBER DRAG COEFFICIENTS WITH EQUATIONS

FILTRATION OF SUBMICRON SIZE AEROSOLS BY FIBROUS MEDIA

by

C. Y. Chen, Research Associate
Chemical Corps Contract No. DA-18-108-CML-4789

The object of this research is to study the filtration of aerosol particles through a fiber mat both theoretically and experimentally. Much work has been done on the development of new filter material and on the measurement of penetration of aerosols through filter material, but not much has been done on the theoretical prediction of the penetration of filter materials and on the experimental study based on the theoretical prediction. The present study is along this line.

THEORY

For filtration of uncharged submicron size aerosols with uncharged filtering medium, the particles might be removed either by inertial impaction, direct interception or Brownian diffusion. To study the filtration of aerosols by fiber mats, it is necessary first to learn the filtration or collection efficiency of a single fiber which composes the mat.

For single fibers, the efficiency of collection of aerosols (η) by any mechanism can be expressed as the ratio of the cross sectional area of the original stream from which particles of a given size are removed because their trajectories intersect the collector surface to the projected area of the collector in the direction of flow. The efficiency of collection by inertia impaction is a function of $\Psi = (C \rho_p d_p^2 v)/(18 \mu d_f)$ and N_{Re}; by direction interception, η is a function of $R = d_p/d_f$ and N_{Re}; and by diffusion, η is a function of $D = D_{BM}/v d_f$ and N_{Re}. The collection by inertial impaction and diffusion increases with Ψ and D, respectively, and always increases with increase of N_{Re}. The importance of direct interception increases with increase of R and decreases with increase of Ψ and D.

Not much experimental work has been done on the collection efficiency of a single fiber especially under the conditions present during the filtration by fiber mats, that is, very low Reynolds number. Until recently, the calculation of collection efficiency by inertial impaction was based on potential flow which can hardly be in the case in the fiber mats when the Reynolds number is usually much less than 1. Davies[1] calculated the inertial impaction and direct interception on fibers assuming viscous flow. From his results, η could be plotted as a function of Ψ with R as a parameter. Davies' results indicated that inertial impaction efficiency based on viscous flow is much lower than that calculated from potential flow. Langmuir[2] has derived equations for predicting the collection efficiency of a single fiber by interception, by diffusion, and by interception and diffusion combined. He derived his equations from Lamb's equation for viscous flow around a cylinder transverse to the flow. Figure 1 shows the collection efficiency by diffusion and interception at a Reynolds number of 10^{-2}.

An interesting conclusion from these calculations is that the collection efficiency due to both effects is higher than the sum of the efficiencies due to the individual effects alone. The same conclusion can be drawn from the Davies calculation of the combined effects of inertial impaction and interception.

The overall efficiency due to inertial impaction, interception and diffusion is very difficult to calculate. A reasonable assumption is that the overall efficiency will be equal to the sum of the efficiencies due to inertial impaction and interception and that due to diffusion and interception. Calculated efficiencies based on this assumption for 2 μ and 3 μ diameter fiber for different particle size and velocity are shown in Figures 2 and 3.

The orientation of fibers in ordinary fiber mats can be considered as lying between two extreme cases. In the first case, the fibers are dispersed uniformly and far apart and the neighboring fibers are staggered with respect to each other. In the second case, the fiber in each layer of mat is lined up to form a group of capillaries. The ordinary fiber mat with high porosity approximates the first case.

In a fiber mat of the first case with porosity approaching 100 percent, all the fibers are available for collection. It is possible to express the overall collection efficiency of this ideal fiber mat as a function of individual fiber total collection efficiency η as defined above.

$$-\ln \frac{N}{N_o} = \frac{4}{\pi} \cdot \eta \cdot \frac{1-\epsilon}{\epsilon} \cdot \frac{L}{d_f} \tag{1}$$

This equation applies only when the fibers are far apart and there are no interference effects between neighboring fibers. Actually, the equation is approximately true for high porosity fiber mats. It is reasonable to express the neighboring fiber interference effect as a function of interfiber distance, or as a function of porosity only for the same type of mat within a narrow range of Rynolds number. Thus, the following equation can be used to express the fiber mat collection efficiency.

$$-\ln \frac{N}{N_o} = \frac{4}{\pi} \cdot \eta \cdot \frac{1-\epsilon}{\epsilon} \cdot \frac{L}{d_f} \cdot F(\epsilon) \tag{2}$$

$F(\epsilon)$ has a limiting value of 1 for mats with porosity of 100 percent; it is greater than 1 when the porosity decreases, and has an asymptotic value for low porosity mats. The function can be calculated from pressure drop measurements across the mat. For a fiber mat with porosity approaching 100 percent with all the fibers transverse to the flow, the pressure drop can be expressed in the following form, based on the Langmuir equation for the drag force of a single cylinder transverse to the flow when N_{Re} is less than one:

$$\Delta p = \frac{16(1-\epsilon)}{2-\ln N_{Re}} \frac{\mu L}{d_f^2 g_c} \tag{3}$$

White [3] has shown that the viscous drag force for a single cylinder in a finite container is higher than that predicted by Lamb's equation for an isolated cylinder. The deviation is a function of the ratio of the distance between the fiber and the container and the fiber diameter. It can be expressed as a function of porosity for fiber mats to account for the effect of neighboring fibers. This function also has a limiting value of one for 100 percent porosity; it increases to an asymptotic value for low porosity mats and will be approximately the same function of porosity used above to describe the neighboring fiber interference effect on collection efficiency. Thus the pressure drop across the fiber mat can be expressed as

$$\Delta p = \frac{16(1-\epsilon)}{2-\ln N_{Re}} \cdot \frac{\mu L}{d_f^2 g_c} \cdot F(\epsilon) \qquad (4)$$

From this discussion, we are able to calculate the penetration of a fiber mat from the physical factors of the mat (thickness, fiber diameter and porosity), the pressure drop across the mat and the collection efficiency of a single fiber calculated for the operating conditions (velocity, particle density and diameter).

It is now possible to show whether a size of maximum penetration exists for a certain fiber mat from the calculation of the single fiber collection efficiency. Table I shows the results for mats of 3μ and 2μ fibers. It is not surprising from the table that the controversy concerning maximum penetration arises. It is simply due to the fact that only a few experiments have been carried out under very limited experimental conditions.

TABLE I. PARTICLE SIZE AT MAXIMUM PENETRATION

Particle density = 1 g./cc.

Average Velocity in mat cm./sec.	For Fiber Size 3 microns d_p microns	For Fiber Size 2 microns d_p microns
0.1	0.52	0.45
1	0.28	0.23
6	0.19	0.16
10	0.15	0.14
40	0.11	0.10
100	0.075	0.070

EXPERIMENTAL

A LaMer-Sinclair type homogeneous liquid aerosol generator was built for this study with DOP as aerosol material. The particle size was measured either by the polarization "Owl", the growth method (4), or by the diffusion battery (5)

depending on the range of the size of the particles. Penetration through the mat was measured by the NRL-E3 pentrometer. Extensive penetration measurements on air-formed B glass fiber mats are in progress. The present mats used contain a wide range of fiber size. Some of the initial experiments indicate that the theory is quite satisfactory.

Table II contains some experimental results compared with the theory assuming the diameter of fiber is 3.5 microns. The actual size of the fibers has a wide range of distribution and the average size is about 3.5 microns.

TABLE II. COMPARISON OF EXPERIMENTAL RESULTS WITH THEORETICAL PREDICTION

B glass fiber mat porosity 98.6%; thickness 1.2 cm.

Aerosol material: DOP; particle size, 0.30 μ

Velocity cm./sec.	η From Expt.	η by calculation based on $d_f = 3.5\,\mu$
26.8	2.29×10^{-2}	2.58×10^{-2}
12.0	2.61	2.38
5.33	2.70	2.76
2.98	2.66	3.16
1.69	3.85	3.48
0.89	4.35	4.18

CONCLUSIONS

From the experimental data available at the present time, the results agree with the theoretical prediction fairly well. Additional experimental work is in progress. The results indicate that the penetration of a fiber mat for the first time can be predicted by theoretical calculation. Also, the development of a new filter material can be made on a scientific basis rather than by a cut-and-try method. The controversy on whether a maximum penetration size exists has been solved by theoretical calculations and the experimental confirmation of the theory will be presented in the near future.

NOMENCLATURE

C = empirical correction for resistance of air to the movement of small particles (at room temperature and atmospheric pressure, $C = 1 + 0.16/d_p$, where d_p is particle diameter in microns).

d_p = particle diameter

v = upstream velocity or average velocity

d_f = fiber diameter

D_{BM} = Brownian diffusion coefficient of aerosol particles

N/N_o = fraction of penetration of aerosol through fiber mat

L = thickness of fiber mat

Δp = pressure drop across fiber mat

g_c = conversion factor, $32.2 \frac{\text{lb. mass x ft.}}{\text{lb. force x sec.}^2}$

$F(\epsilon)$ = a function of porosity representing neighboring fiber interference effect

D = diffusion parameter, $\frac{D_{BM}}{v\, d_f}$

R = interception parameter, d_p/d_f

Ψ = inertia parameter $\frac{C\rho_p\, d_p^2\, v}{18\, \mu\, d_f}$

ρ_p = particle density

ρ = fluid density

μ = fluid viscosity

η = collection efficiency of a single fiber

ϵ = porosity of fiber mat

LITERATURE CITED

1. Davies, C. M., Preprint, Inst. of Mech. Eng. (London) July 1, 1952.
2. Langmuir, I., OSRD Report No. 865 (1942).
3. White, C. M., Proc. Royal Soc. (London) A186, 472 (1946).
4. LaMer, V. K., Final Report NYO-512, Contract AT-(30-1)-651. (June 1951).
5. DeMarcus, W., Thomas, J. W., ORNL-1413 (Oct. 1952).

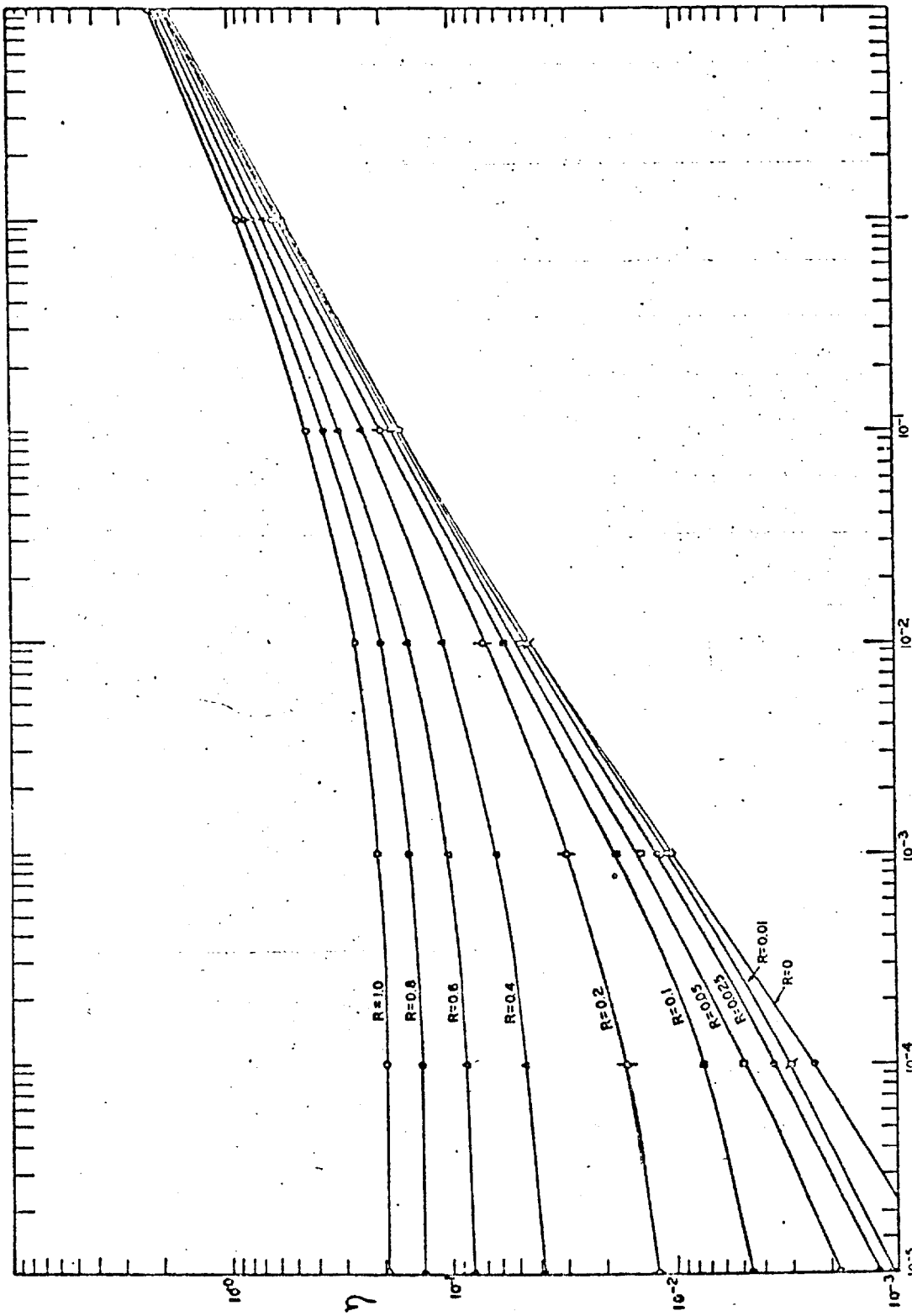

FIG. 1. COLLECTION EFFICIENCY OF A SINGLE CYLINDER BY DIFFUSION AND INTERCEPTION, $N_R = 10^{-2}$

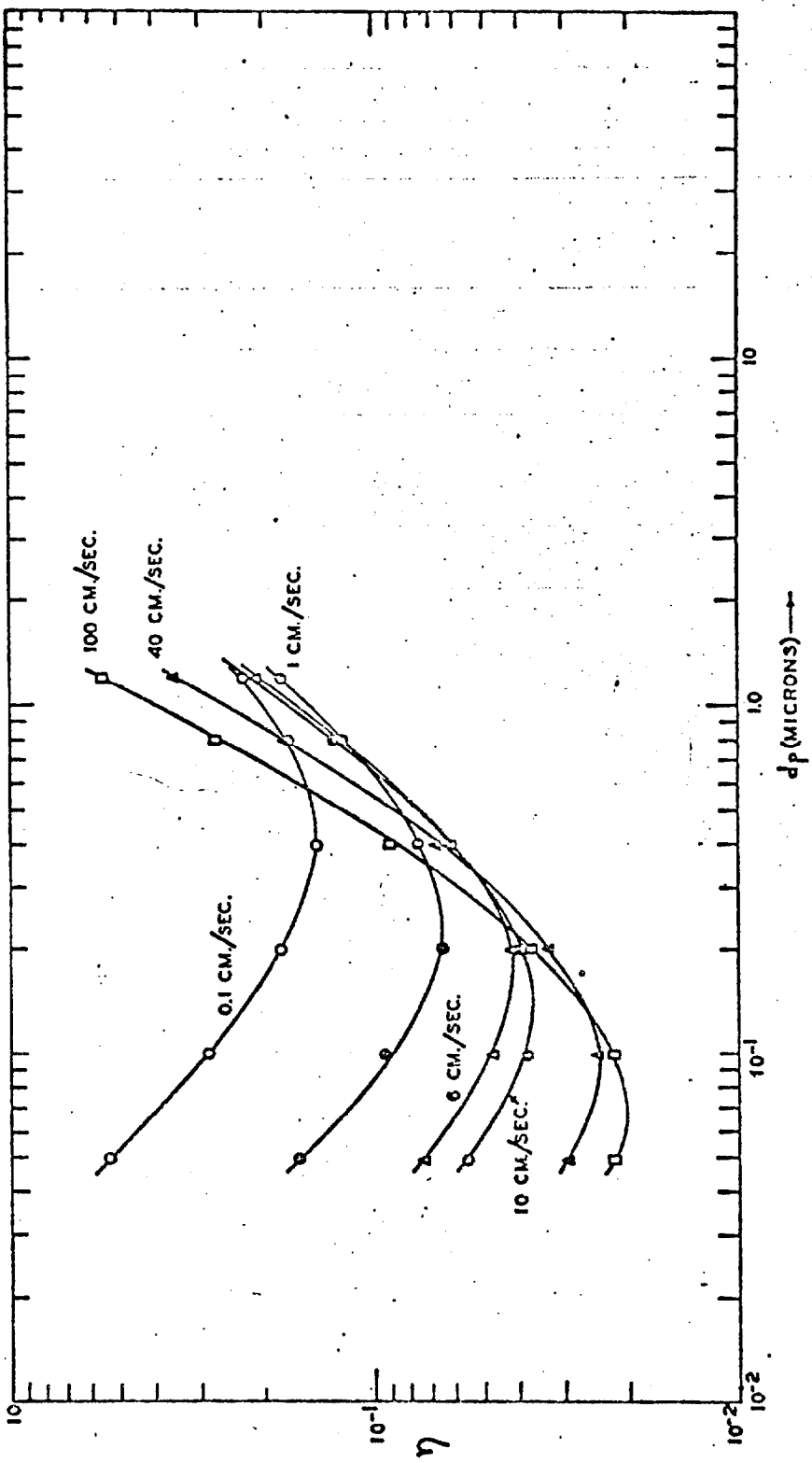

FIG. 2. COLLECTION EFFICIENCY OF 2μ FIBER, PARTICLE DENSITY 1G./CC.

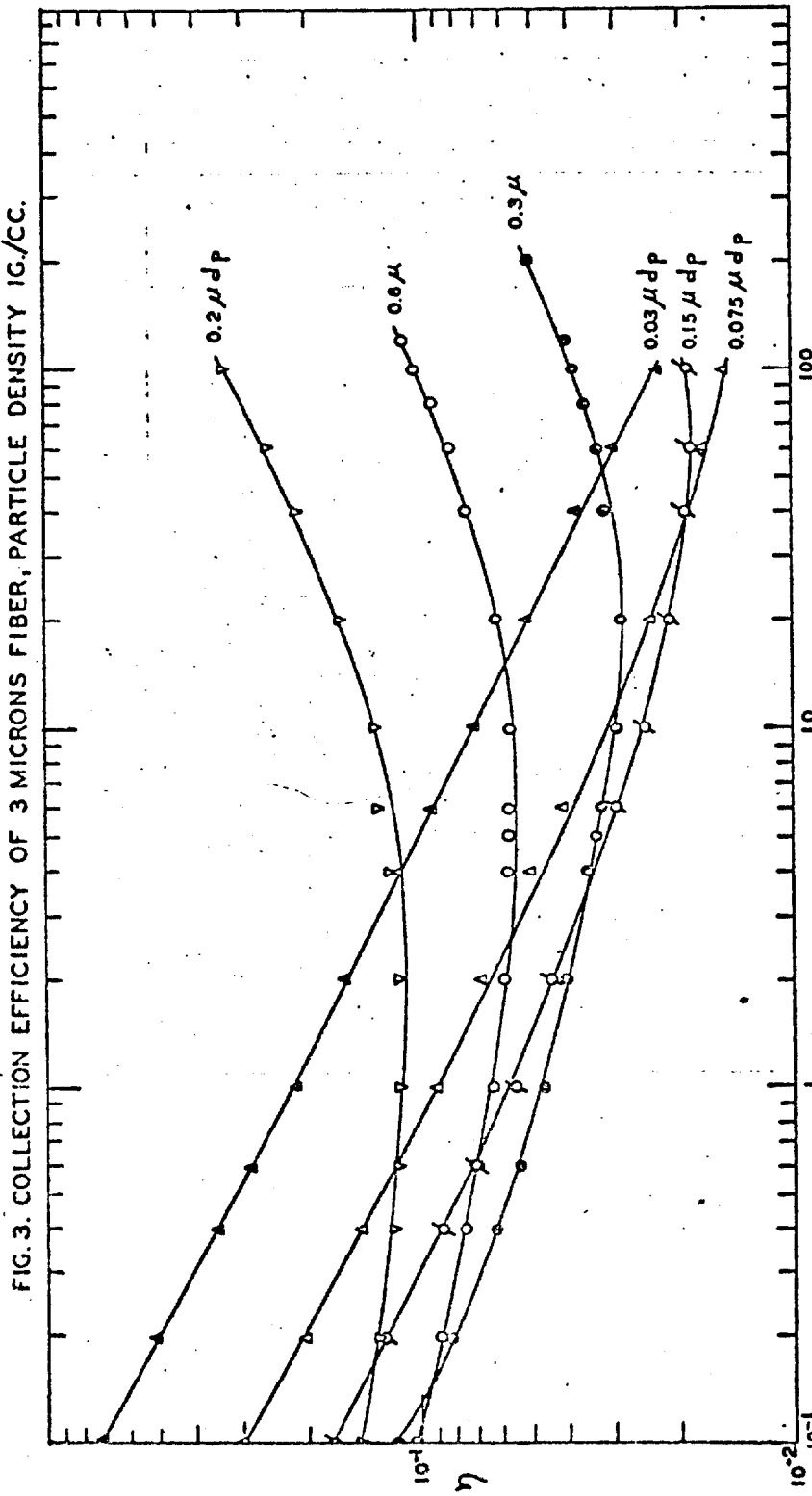

FIG. 3. COLLECTION EFFICIENCY OF 3 MICRONS FIBER, PARTICLE DENSITY IG./CC.

INFLUENCES OF ELECTROSTATIC FORCES ON THE DEPOSITION OF AEROSOLS

by

H. F. Kraemer
Ethyl Corporation Fellow in Chemical Engineering

In recent years several studies have been made on the mechanisms by which particulates can be removed from an aerosol. Although emphasis has been placed on the inertial mechanism of collection, the effects of small electrostatic charges on the aerosol particles and on the collecting surface must not be overlooked in promoting the collection efficiency. Many natural aerosols are electrically charged, as are some collecting surfaces such as the fibers in a resin-wool filter. Uncharged surfaces or aerosols readily can be given an electric charge, thereby increasing the separation of particles from the aerosol.

The utilization of electrostatic forces in promoting aerosol deposition may be advantageous in several ways. The foremost advantage is the high collection efficiency (based on projected cross-sectional area of the collector) that is possible. Although a collection efficiency of more than 100 percent is not possible when only inertial forces are used, efficiencies of 10,000 percent or higher may be achieved if both the collector and the aerosol are charged.* The collection efficiency using electrostatic forces remains high even for submicron particles, although inertial forces in this case may be negligible. Another consideration is the fact that electrostatic mechanisms of collection require low aerosol velocities of flow across the collecting surface. The pressure drops in the system consequently will be much lower than would be the case for similar collection by the inertial mechanism.

The purpose of the current research is to investigate the mechanisms of aerosol deposition under the influence of electrostatic forces and to indicate the conditions and types of equipment wherein electrical charging may be beneficial.

THEORY

Studies are being made of the motion of a charged aerosol particle flowing past a single spherical collector Figure 1. The collection efficiency can be calculated theoretically if the outermost limiting trajectory is known for the aerosol particles just grazing the collector.

The differential equations of motion of a single aerosol particle approaching the spherical collector are given in Figure 2. The equations are derived from force balances of the fluid resistance and of the electrostatic forces of

*The collection efficiency is defined as the fraction of the aerosol removed from a tube of gas subtended by the collecting obstacle as the gas flows past.

attraction between (1) a charged collector and a charged aerosol (parameter K_E), (2) a charged collector and its image in an uncharged aerosol particle (parameter K_I), (3) a charged aerosol and its image in an uncharged collector (parameters K_M and K_S). The several electrostatic forces can be shown to be approximately additive. Potential flow streamlines and Stokes' law are also used in deriving the equations. Since the differential equations have been made dimensionless, all of the experimental variables are contained in the dimensionless parameters K_E, K_I, K_M, K_S Figure 3.

Although the solution of the two simultaneous differential equations is possible only by a numerical method, order of magnitude solutions may be obtained by ignoring the bending of the air streamlines around the spherical collector and by considering only one collection parameter, K_E, K_I, K_S or K_M, at a time.

The numerical solution of the trajectory equations has been completed by means of the electronic digital computer, the ILLIAC. Collection efficiencies were calculated for a range of values of the four parameters, K_E, K_I, K_S and K_M. Some of the results are shown in Figure 4.

In order to interpolate between solutions obtained with the computer, the collection efficiencies and the collection parameters may be correlated by curve-fitting with a high-order multivariate polynomial.

EXPERIMENTAL EQUIPMENT AND PROCEDURE

The equipment is shown in Figure 5. A dioctylphthalate (DOP) fog is produced by condensation of the vapor in the presence of salt nuclei. The particle diameter is about 0.8 ± 0.2 micron. The aerosol is charged electrically by passing it through coaxial electrodes in a state of corona. Charges of +10 to +80 electronic units can be obtained. A description of the mechanism of the charging process and of the method of measuring the charges on the aerosol particles was given at the Ames Conference in 1952.

The charged aerosol then flows past the spherical collector which is a 7/16" steel ball mounted on the end of a semi-conducting cone. The cone acts as an electrostatic shield around the wire connecting the sphere to a high voltage D.C. power supply (0-10,000 volts). Without it, the electric charge on the wire affects the collection on the sphere.

The electrical charge on the aerosol is determined from the deflection of a streamer of aerosol flowing in a transverse electric field. The aerosol is carried through the field by an envelope of moving air. The size of the particles is measured by the "Owl" and by a high velocity cascade impactor. The mass concentration of the aerosol is determined by precipitation of a sample in a small glass and platinum Cottrell precipitator.

The collection efficiency is determined experimentally by measuring the amount of aerosol deposited on the sphere and in the sampling Cottrell precipitator. The DOP is removed from the collecting surfaces by washing with ethyl alcohol and the concentration found by ultra-violet spectrophotometry. Collection on the sphere ranges from 1 to 10 micrograms of DOP per minute.

EXPERIMENTAL RESULTS

The preliminary data are shown in Figures 6 and 7. The inertial parameter Ψ is about 10^{-6}. According to theory, the inertial forces should therefore have a negligible effect on the deposition.

The actual collection agrees approximately with that predicted by theory. In the case of the uncharged aerosol flowing near a charged collector, the data have a high experimental variability on account of the small amounts of DOP that were collected and measured.

In Figure 7 the data are plotted versus a modified parameter. Whenever a collector is grounded, even through a high resistance, charges are induced on the collector by all the surrounding charged particles. This induced charge occurs in addition to the image and void space effects described by the parameters K_M and K_S. The induced charge is calculated by an integration process and its contribution to deposition is combined with that of the K_S parameter. The combined parameter is K_S. Figure 7 illustrates data in which the induced charge resulting from grounding the collector was the major factor influencing deposition.

PRELIMINARY CONCLUSIONS

A practical application of electrostatic forces is illustrated in the use of charged water droplets for collection of aerosol particles which themselves are charged by passage through a corona discharge. An electrified wet scrubber would have several advantages over both the conventional wet cyclone and the Cottrell precipitator. Compared to a conventional scrubber, the electrified scrubber should provide better removal of submicron aerosol particles. Conversely, it would require less water and could operate at lower velocities and pressure drops for the same efficiency of aerosol removal. Furthermore, it would have several advantages over the Cottrell precipitator. The precipitated material would be removed continuously on the surfaces of the spray droplets, thereby eliminating the problems often encountered in precipitating dusts that have a tendency for reentrainment. The retention time in an electrified scrubber would be lower than in a Cottrell precipitator because an aerosol particle must travel a shorter distance to the nearest spray droplet. Also, the electrified scrubber would be operated at relatively lower voltages (1000 to 10,000 volts) since the collection distances are smaller.

An electrified spray scrubber is now being constructed to evaluate its potentialities.

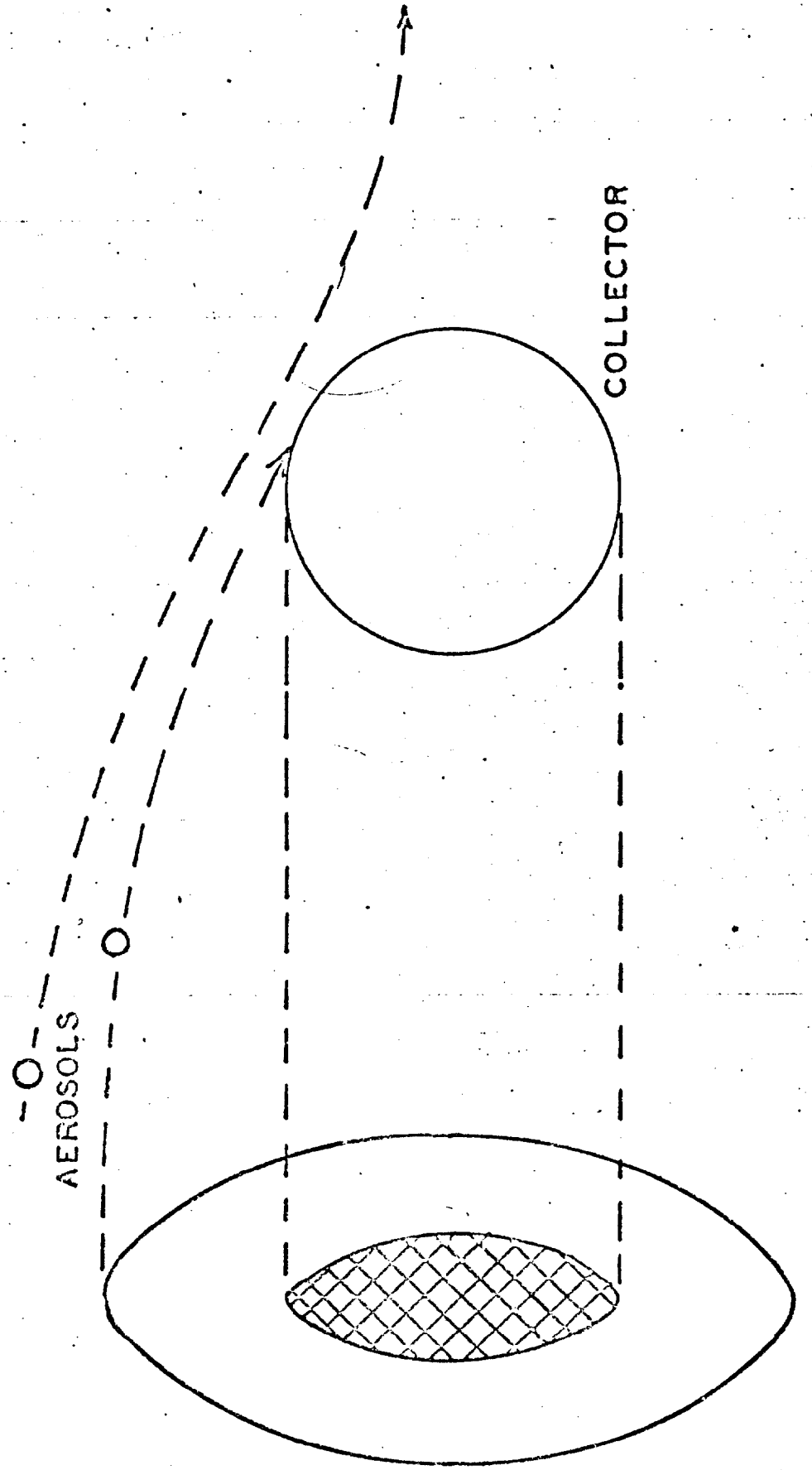

FIG. 1 – TRAJECTORY OF AEROSOL PARTICLE UNDER INFLUENCE OF ELECTROSTATIC CHARGE ON COLLECTOR

Angular Velocity of Aerosol Particle

$$\frac{d\theta}{dt} = -\frac{(2r^3 + 1)}{2r^4} \sin\theta$$

Radial Velocity of Aerosol Particle

$$\frac{dr}{dt} = \frac{(r^3 - 1)}{r^3} \sin\theta - \frac{(K_E + K_S)}{r^2} - \frac{K_I}{r^5} - K_M \left(\frac{r}{(r^2 - 1)^2} - \frac{1}{r^3} \right)$$

FIGURE 2 - DIFFERENTIAL EQUATIONS OF TRAJECTORY OF AEROSOL PARTICLE

Potential Flow with Electrostatic Forces and
Stokes' Resistance

$$K_E = \frac{q_p\, q_{ac}\, C}{3\pi\mu D_p\, v_o\, \epsilon_o}$$

Coulombic attraction

$$K_S = \frac{q_p^2\, n\, D_c\, C}{18\pi\mu D_p\, v_o\, \epsilon_o}$$

Repulsion by surrounding aerosol

$$K_I = \frac{2(\epsilon - 1)\, D_p^2\, q_{ac}^2\, C}{3(\epsilon + 2)\,\mu v_o\, \epsilon_o D_c}$$

Image force of charged collector on uncharged aerosol

$$K_M = \frac{q_p^2\, C}{3\pi^2\mu D_p\, v_o\, \epsilon_o\, D_c^2}$$

Image force of charged aerosol on uncharged collector

FIGURE 3 - ELECTROSTATIC COLLECTION PARAMETERS

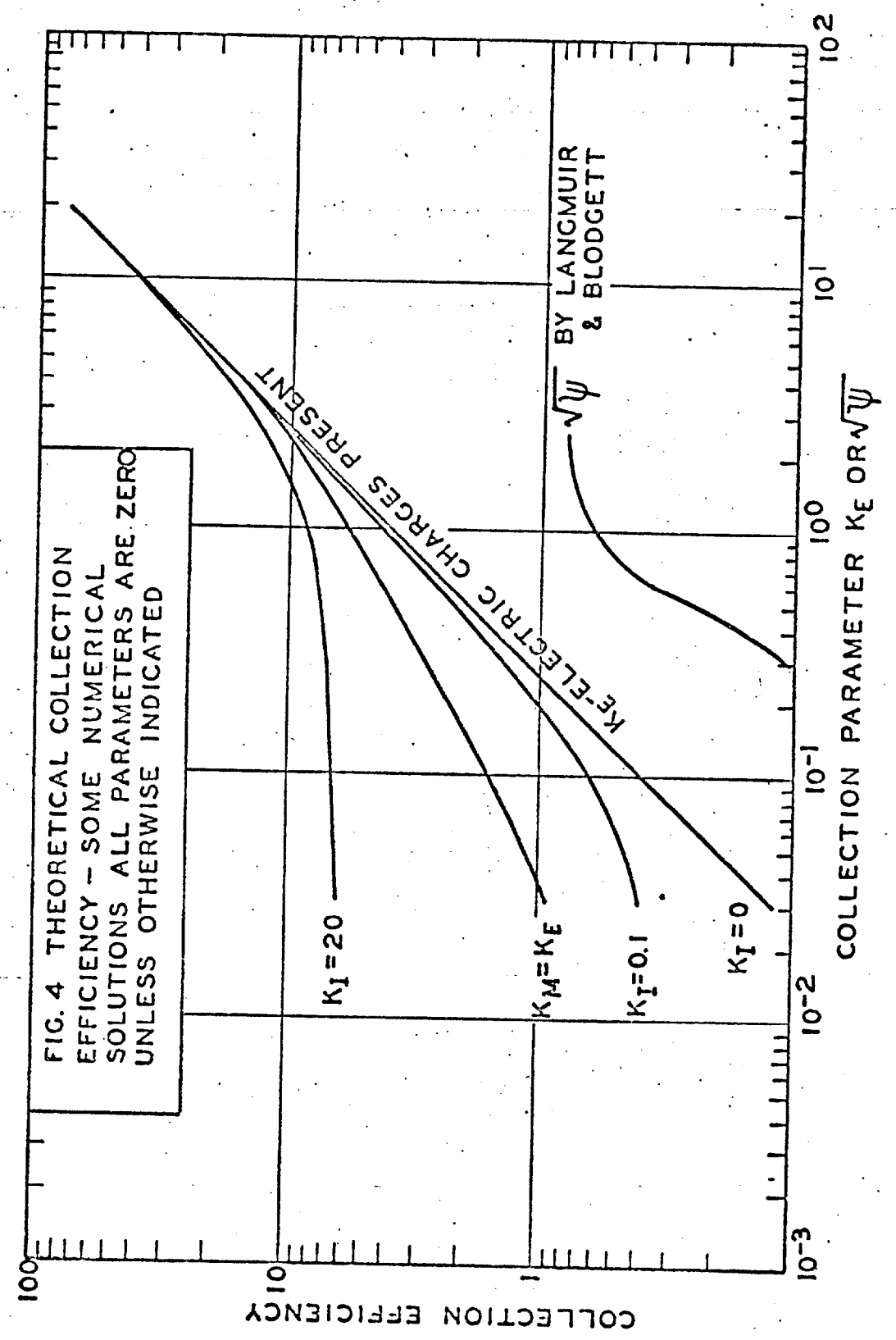

FIG. 4 THEORETICAL COLLECTION EFFICIENCY – SOME NUMERICAL SOLUTIONS ALL PARAMETERS ARE ZERO UNLESS OTHERWISE INDICATED

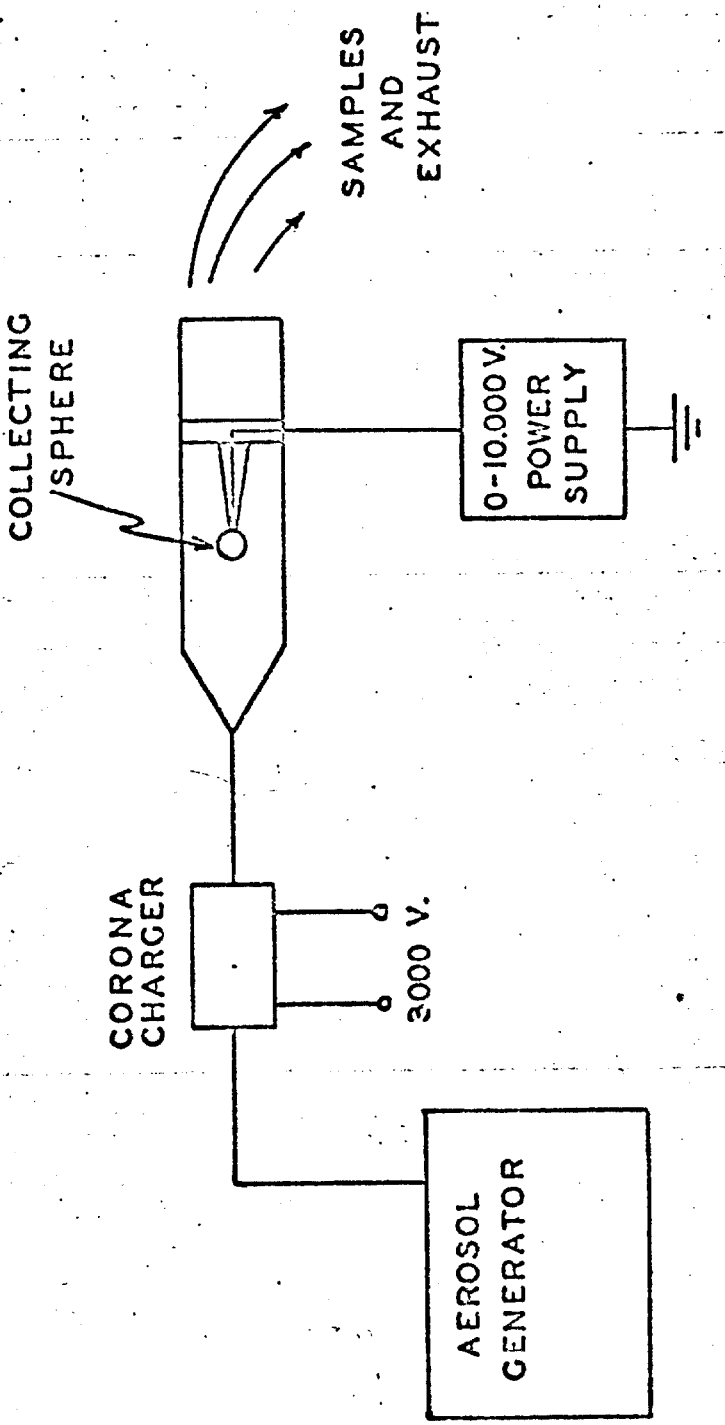

FIG. 5 - FLOW DIAGRAM OF EXPERIMENTAL EQUIPMENT

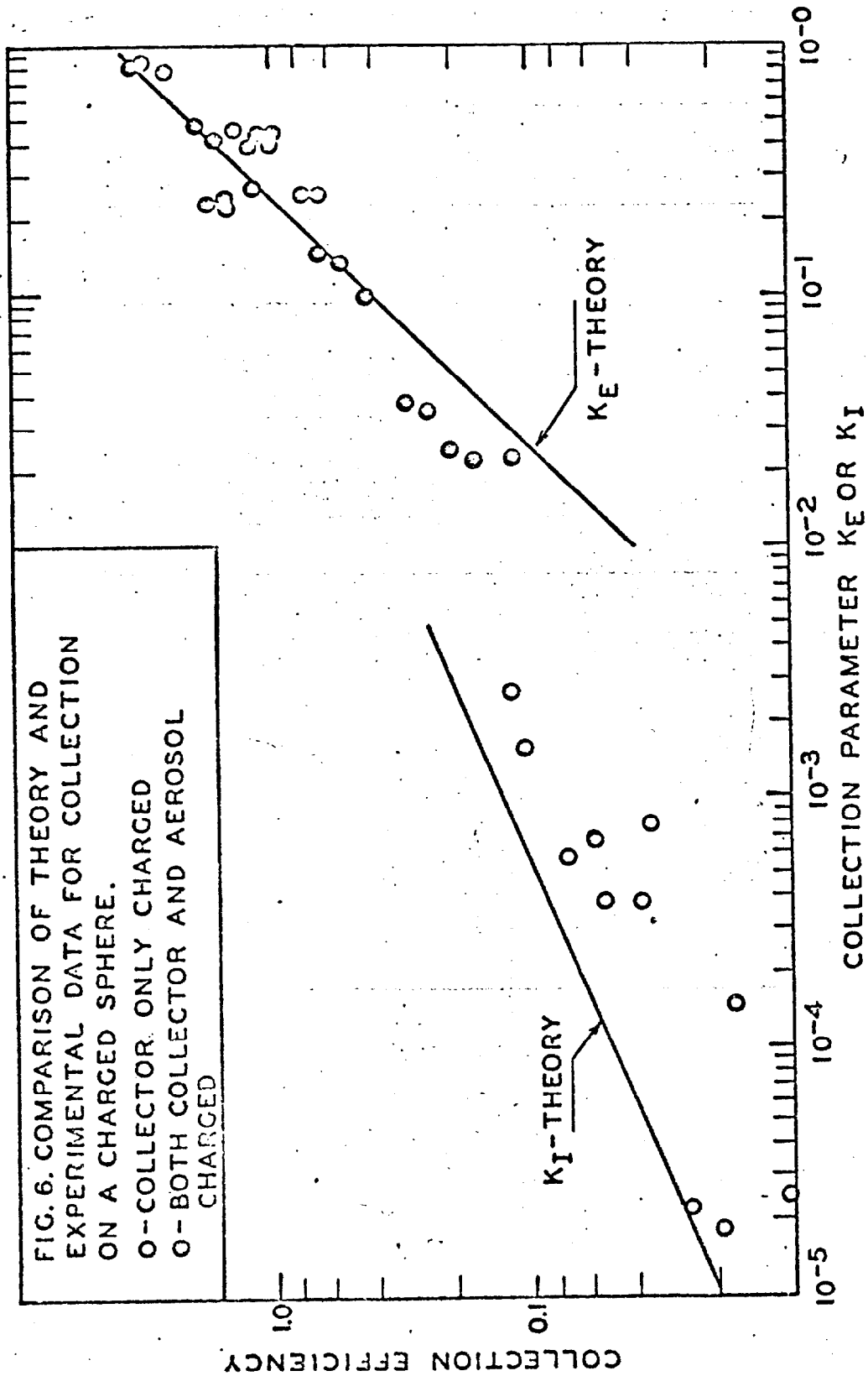

FIG. 6. COMPARISON OF THEORY AND EXPERIMENTAL DATA FOR COLLECTION ON A CHARGED SPHERE.
O - COLLECTOR ONLY CHARGED
O - BOTH COLLECTOR AND AEROSOL CHARGED

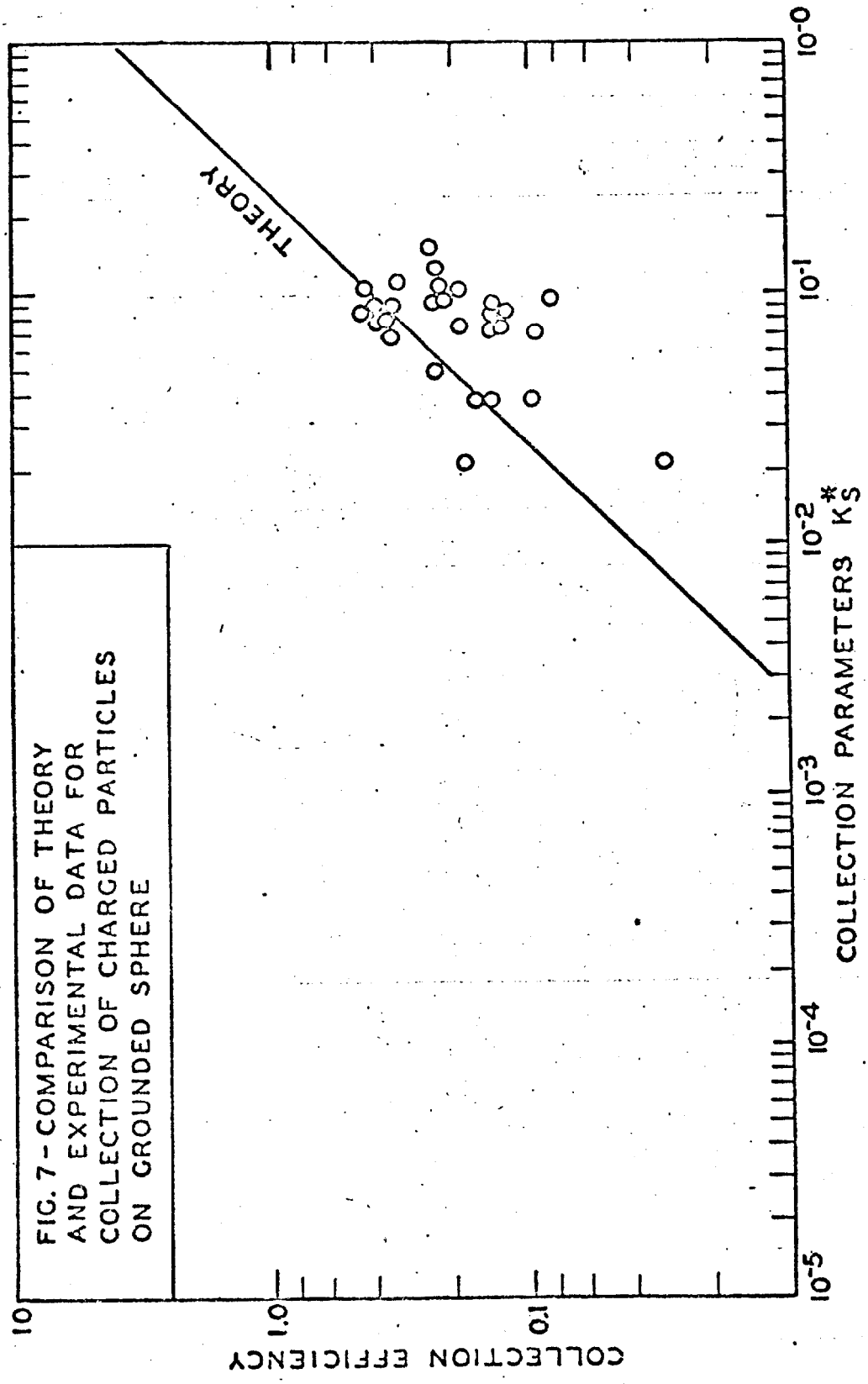

FIG. 7 - COMPARISON OF THEORY AND EXPERIMENTAL DATA FOR COLLECTION OF CHARGED PARTICLES ON GROUNDED SPHERE